High-Contrast Solid-State Electrochromic Devices of Viologen-Bridged Polysilsesquioxane Nanoparticles Fabricated by Layer-by-Layer Assembly

Vaibhav Jain,[†] Mariya Khiterer,[‡] Reza Montazami,[§] Hank M. Yochum,[||] Kenneth J. Shea,[‡] and James R. Heflin*,[⊥]

Departments of Macromolecular Science and Engineering, of Materials Science and Engineering, and of Physics, Virginia Tech, Blacksburg, Virginia 24061, Department of Chemistry, University of California, Irvine, California 92697, and Department of Physics and Engineering, Sweet Briar College, Sweet Briar, Virginia 24595

ABSTRACT Water-soluble silsesquioxane nanoparticles (NPs) incorporating viologen groups (PXV; 1,1′-bis[3-(trimethoxysilyl)propyl]-4,4′-bipyridinium iodide) have been synthesized by sol−gel polymerization. The electrochromic properties of the bulk film fabricated by layer-by-layer (LbL) assembly have been examined, along with their incorporation into solid-state devices. The orange LbL films show high thermal stability and exhibit a maximum UV−vis absorption at 550 nm. Electrochromic switching of the NPs in liquid electrolyte as well as in the solid state was evaluated by a kinetic study via measurement of the change in transmission (% T) at the maximum contrast. Cyclic voltammograms of the PXV NP LbL films exhibit a reversible reduction at −0.6 V vs Ag/AgCl in a 0.1 M $NaClO_4$(aq) solution, revealing good electrochromic stability, with a color change from orange to dark purple-blue at applied potentials ranging from −0.7 to −1.3 V. Cathodically coloring PXV NP solid-state devices exhibit a switching time of a few seconds between the purple-blue reduced state and the orange oxidized state, showing a contrast of 50% at 550 nm and a coloration efficiency of 205 cm^2/C. Their solubility and fairly fast electrochromic switching (~3 s) at low switching voltages (between 0 and 3.0 V), along with their stability under atmospheric conditions, make PXV NPs good candidates for electrochromic displays.

KEYWORDS: polyviologen • layer-by-layer • polysilsesquioxanes • conjugated polyelectrolyte • electrochromic devices

INTRODUCTION

Electrochromic materials change color as a result of oxidation or reduction when an appropriate electric potential is applied (1). The electrochromic properties of viologens are well documented and have received significant attention for the past 35 years because of their electrical and electrochromic properties and good environmental stability (2−5). With the exception of TiO_2 microparticles modified with viologen pendants (6), all of these reports, however, describe electrodeposited or polymeric thin films of 1,1′-substituted 4,4′-bipyridinium salts. Electrochromic devices incorporating viologen nanoparticles (NPs) have not been previously reported. The main advantage of using nanoparticulate electrochromic materials is the large surface area that they afford. This allows for high color contrast ratios in very thin devices suitable for such display technologies as flexible electronic paper at very low charge transfer, which yields higher coloration efficiency (CE) (7, 8). In addition, the porosity of films prepared from spherical electrochromic NPs can enhance the response time of an electrochromic device because of improved ionic conductivity (9). The authors of this article have recently described the first synthesis of viologen-bridged polysilsesquioxane spherical NPs (10). Suh (11) and Neoh (12) et al. have shown the fabrication of viologen-functionalized polymeric micro- and nanospheres, respectively. Suh et al. have also shown the application of monodispersed, micrometer-size-range polymeric microspheres with different lengths of the viologen pendant group in reflective electrochromic devices as well (13). Improvement in the switching speed (<1 s) with a significant drop in contrast (<30%) was observed, but the overall device fabrication is tedious and a thin film device with long-term stability (>10 000 cycles) is a distant possibility (14).

The most common techniques to deposit electrochromic polymers on electrodes are spin coating (15), thermal evaporation (16), surface polymerization by chemical means (17), and electropolymerization (18), but the layer-by-layer (LbL) film fabrication method gives a fine degree of control to optimize the capabilities of electrochromic films (19, 20). LbL deposition of polymeric thin films is a technique developed by Decher et al. (21, 22), and Kotov et al. (23) were the first to introduce NPs in the LbL fashion. Several other groups have also done pioneering work in studying various aspects of NP LbL assembly, making it one of the most promising

* To whom correspondence should be addressed. E-mail: rheflin @vt.edu. Tel: 540-231-4504. Fax: 540-231-7511.
Received for review August 28, 2008 and accepted November 25, 2008
[†] Department of Macromolecular Science and Engineering, Virginia Tech.
[‡] University of California.
[§] Department of Materials Science and Engineering, Virginia Tech.
[||] Sweet Briar College.
[⊥] Department of Physics, Virginia Tech.
DOI: 10.1021/am8000264

new methods of thin film deposition of NPs (24–26). LbL assembly is done by alternately dipping a substrate into solutions of polycations and polyanions, which often results in linear film growth, with the ultimate thickness being controlled by the number of bilayers deposited. The main advantage of adopting the LbL technique over Langmuir–Blodgett (LB) multilayers is that the electroactivity decreases quickly as the number of layers is increased, disappearing after three to four layers in the case of LB films, whereas the film deposited by the LbL method remains highly electroactive even after deposition of 80 layers (27).

Bridged polysilsesquioxanes (BPSs) are hybrid network materials that have organic and inorganic domains dispersed at the molecular level (28–30). Because the organic group remains an integral component of the material, this variability provides an opportunity to modulate bulk properties such as porosity, thermal stability, refractive index, optical clarity, chemical function, hydrophobicity, and dielectric constant. The organic component not only strongly contributes to the bulk physical properties but also provides functionality to the materials. The fine degree of control over the bulk chemical and physical properties has made these materials candidates for applications in optical devices (31–35), as high-capacity absorbents (36–38), 3D information storage media (39), and proton-conducting media for fuel cells (40, 41).

Work related to polysilsesquioxane (POSS) in electrochromic devices is quite new. Lu et al. have shown the importance of porosity and facile ion diffusion of POSS (42). Although the results are interesting, the nanosized POSS in their work is not water-soluble, has a long switching time with low CE, and results in a significant red/blue shift during spectroelectrochemical measurements. Conversely, we have shown high-contrast, fast-switching electrochromic devices of water-dispersed BPS NPs fabricated by the bottom-up LbL assembly technique, where a combination of BPS NPs with other contrast-enhancing electrochromic material is also possible.

Here, we report the use of these NPs in LbL electrochromic devices with poly[2-(acrylamido)-2-methyl-1-propanesulfonic acid] (PAMPS). To improve the contrast in the system, we preferred PAMPS at a very low weight percentage [4.125×10^{-2}% w/w (2 mM) in water] as a polyanion in the LbL film assembly because of its natural ability to transfer ions and the fact that it provides less bulk resistance and faster color change. The bilayers were characterized by cyclic voltammetry (CV), X-ray photoelectron spectroscopy (not shown), UV–vis spectroscopy, transmission spectra in a solid-state device, and morphological studies by atomic force microscopy (AFM). In this study, we measured the electrochromic switching response of 1,1′-bis[3-(trimethoxysilyl)propyl]-4,4′-bipyridinium iodide (PXV) NP films in solid-state devices, which are composed of a PXV NPs/PAMPS film on indium tin oxide (ITO) slides sandwiched with another ITO slide containing a LbL film of polyaniline (PANI)/PAMPS (Scheme 1).

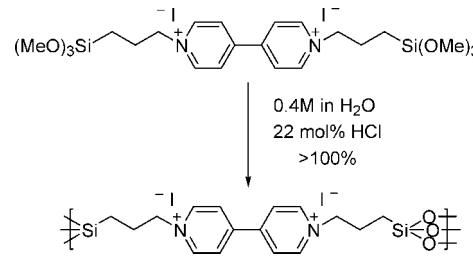

FIGURE 1. Sol–gel polymerization of PXV.

Scheme 1. LbL Deposition of PXV NPs on the ITO Electrode

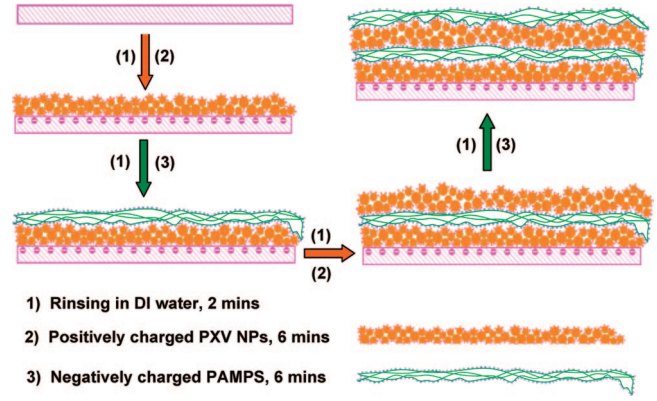

RESULTS AND DISCUSSION

NP Synthesis. The NPs described herein were prepared by inverse water-in-oil microemulsion polymerization (43, 44). The details of this method are described elsewhere (10). Briefly, the emulsions were prepared using NP-5 as the surfactant and 1-hexanol as the cosurfactant to disperse 0.4 M aqueous PXV solutions in cyclohexane. PXV was prepared from 3-iodopropyltrimethoxysilane and bipyridyl according to a published procedure by Bookbinder and Wrighton (45). Here, each microemulsion droplet acts as a "container" where the sol–gel reaction takes place (Figure 1).

After addition of the catalyst (HCl), the emulsions were allowed to age for 48 h to provide time for the formation of stable, solid BPS gel particles. The particles were precipitated with ethanol and washed with water to remove residual surfactant. To determine the particle size and distribution, wet gel particle microemulsions were analyzed by dynamic light scattering. The samples were also drop-deposited onto silicon wafer substrates, allowed to dry over a period of 24 h, and then analyzed by scanning electron microscopy (SEM; Figure 2).

The SEM image and its corresponding size distribution (parts A and B of Figure 2, respectively) reveal that the particles are spherical and relatively monodisperse in size with an average diameter of 43 ± 8 nm. The light scattering data of the microemulsion prepared under the same conditions (Figure 2C) shows a monomodal distribution centered around 120 ± 36 nm. The smaller average particle size of the SEM data compared to the wet gel diameters is due to a 95% volume drop upon drying to a xerogel, normal for BPSs prepared under these conditions. The internal structure of the BPS NPs was investigated using TEM (Figure 3). The material was found to be uniform and featureless with no

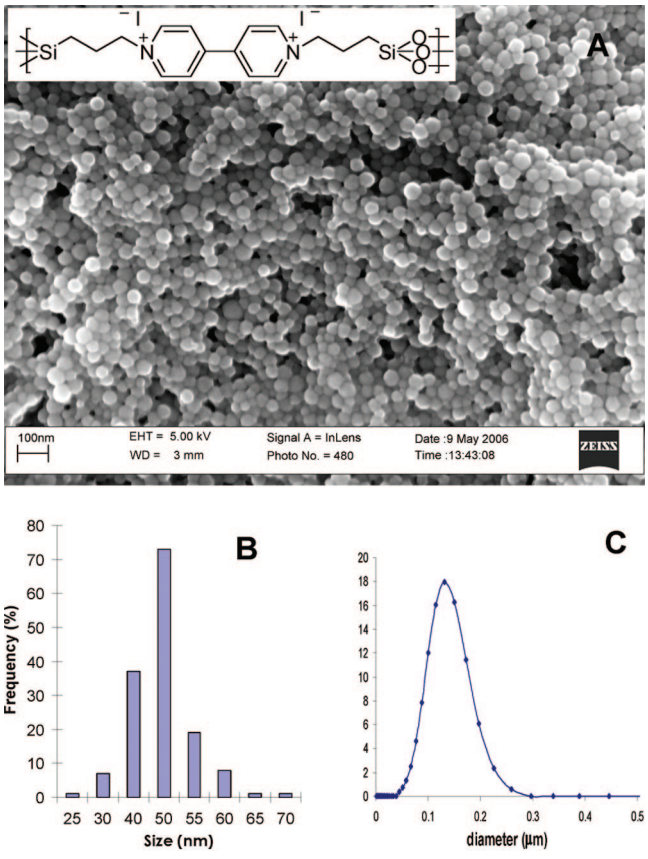

FIGURE 2. PXV BPS NPs: (A) SEM micrograph of dried xerogel; (B) size distribution of the particles in A; (C) size distribution of wet gel particles in a microemulsion.

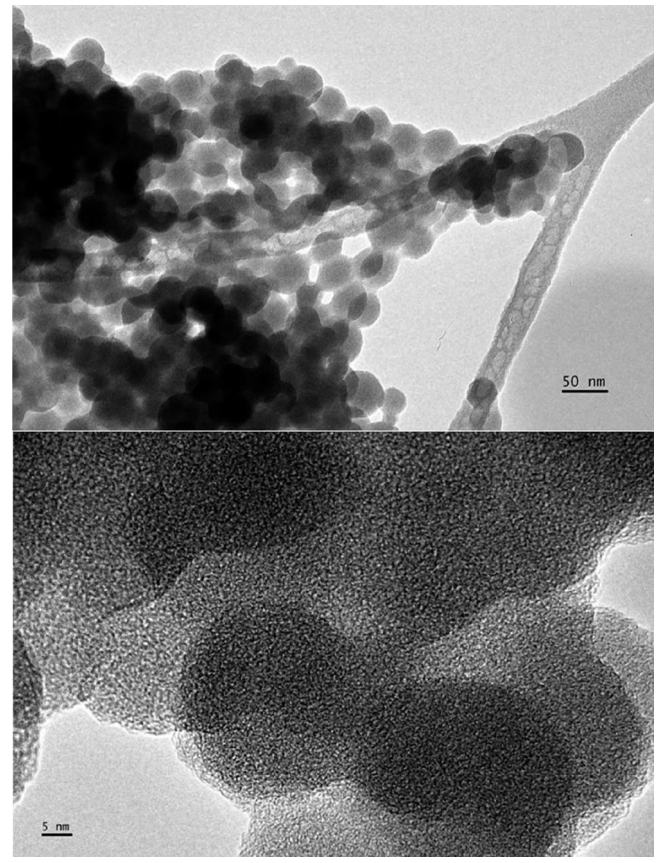

FIGURE 3. TEM of BPS NPs prepared from PXV.

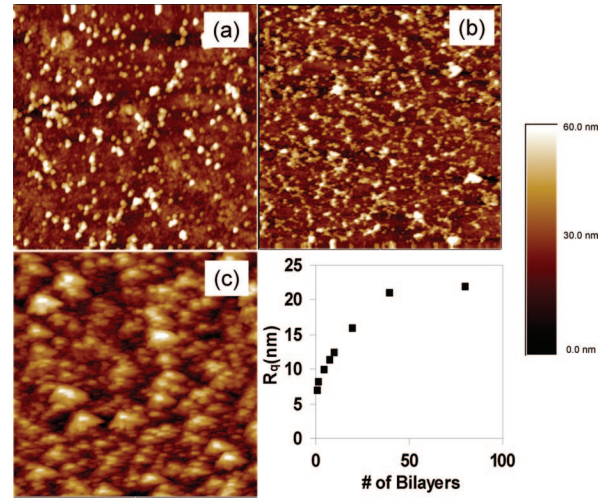

FIGURE 4. AFM images of different numbers of bilayers of PXV/PAMPS LbL films: (a) 2, (b) 5, (c) 10, and (d) surface roughness variation with the number of bilayers.

apparent phase separation or long-range order. The ζ potential value of the BPS NPs was measured to be +48.6 mV.

Surface Analysis. Morphological studies of different numbers of PXV NPs/PAMPS bilayers on an ITO electrode by AFM (Figure 4) and SEM (Figure 5) reveal that the LBL films are conformably coated onto the surface. AFM scans of several LbL films confirmed the nanoporous morphology and showed that the surface roughness initially increases as the number of bilayers increases but plateaus in the range of 22 nm for 40 bilayers or more. For the first few bilayers (two and five, as seen in Figure 4a,b), the LbL film consists of isolated 3D clusters of many NPs. However, upon subsequent deposition of additional bilayers (Figure 4c), the film becomes thicker and more homogeneous with fairly large aggregates of NPs distributed covering the entire surface.

The increase in the surface roughness is from the large surface area of the PXV NPs, which, in turn, increases the surface area of the LbL film by depositing an increasing amount of material with subsequent depositions. As NPs are deposited in each bilayer, the surface roughness stops increasing linearly and plateaus after 40 bilayers or so.

This phenomenon, also observed by other groups, happens when the repulsion and attraction both remain strong, while balancing each other, promoting uniform deposition with similar surface roughness (46).

Solid-State Devices. The fabrication of solid-state electrochromic LbL devices has been described in one of our recent publications (47). In brief, "asymmetric" solid-state devices are fabricated by pressure-laminating two LbL films with different materials coated on ITO electrodes with a few drops of PAMPS gel placed in between with the help of paper clips for 20 min and then sealing the ends with the epoxy so that PAMPS does not quickly evaporate; the overall device configuration is shown in Scheme 2. 40-bilayer films of PXV NPs/PAMPS and PANI/PAMPS on ITO act as the working electrode and the counter electrode, respectively. It was found that a "symmetric" polyviologen/PAMPs−polyviologen/

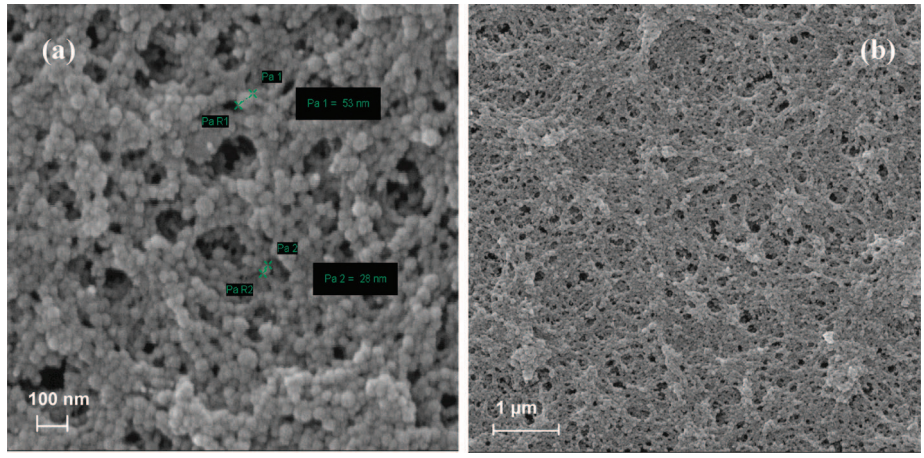

FIGURE 5. SEM images of (a) 20 and (b) 40 bilayer films of PXV NPs/PAMPS.

Scheme 2. Asymmetric Solid-State Electrochromic Device from LbL Films of 40 Bilayers of PXV NPs/PAMPS and PANI/PAMPS

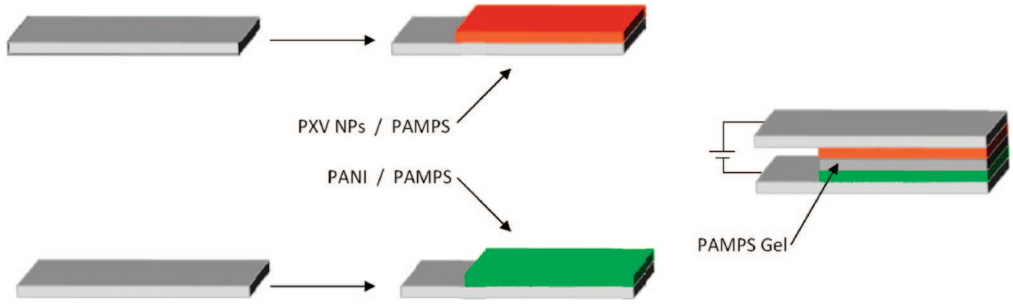

PAMPS sandwich did not have any color change with an applied voltage, while the polyviologen/PAMPS−PANI/PAMPS devices did show a color change at the region similar in wavelength (~550 nm) to that of a polyviologen/PAMPS film in a liquid electrolyte solution. In addition, we have shown in our previous work that the PANI/PAMPS color change (green to blue) is maximum at 500 nm (48), which confirms that the color change in the asymmetric solid-state device at 550 nm is from PXV NPs and not from PANI. The PAMPS component of these films is not electrochromic. The polyelectrolyte gel used in fabricating the solid-state device is also PAMPS (35% in H_2O) and has been commonly used for electrochromic device fabrication by ours and a few other groups (49, 50).

CV. CV was performed on a 40-bilayer film of polyviologen NPs/PAMPS (Figure 6a), which is similar to those of the polyviologen-containing LbL films studied by Delongchamp et al. (20) and self-assembled monolayers of Ock et al. (51) A sharp peak appears at −0.7 V, corresponding to the first reduction, and the resulting monocationic radical appears as a deep-purple color. The purple color remains during the reduction scan between −0.7 and −0.9 V but changes to pale yellow because of the doubly reduced viologen at potentials higher than −0.9 V. During the oxidation scan, the color changes from pale yellow to deep purple and finally back to the original transparent state. One important feature of these data is that the peak potentials for both reduction and oxidation have shifted to more negative and less positive values, respectively with respect to the ones at lower scan rates. This phenomenon is attributed to the internal resistance of the bulk film and has been described previously (20, 52, 53).

The peak current density varies linearly with the square root of the scan rate for both oxidation and reduction (Figure 6b), which confirms that the redox process is diffusion-controlled and the whole film contributes to the change in color. This is one of the primary reasons that we observe such a high color contrast from the contribution of polyviologen alone. Diffusion-controlled redox is significant for the long-term stability of electrochromic devices because it prevents charge trapping and film degradation with time, as is observed with surface-controlled redox processes (20). So, the entire thin LbL film is accessible in this case and allows the maximum contrast possible for the polyviologen. CV was done for films of different numbers of bilayers, and for all multilayer films, the diffusion-controlled redox process remained constant.

Spectroelectrochemistry. *Optical Switching in a 0.1 M $NaClO_4$(aq) Solution.* A 40-bilayer film of PXV NPs/PAMPS on ITO in a 0.1 M $NaClO_4$ electrolyte showed a contrast of about 50% at 550 nm wavelength (Figure 7). The color of the film changes from orange (color of NPs) in the bleached state to dark purple-blue (reduction at −0.7 V) to transparent yellow (−1.3V) upon complete reduction of the bipyridinium dication. It is important to note that similar to most other electrochromic materials the PXV NP film does not exhibit a memory effect in the liquid

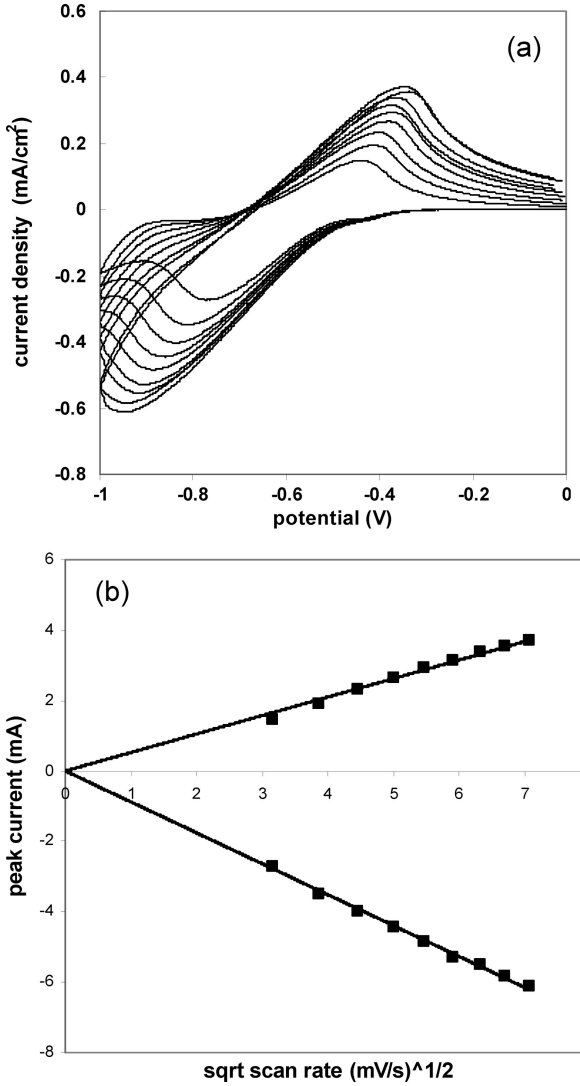

FIGURE 6. (a) CV of a 40-bilayer PXV NPs/PAMPS film in 0.1 M $NaClO_4$(aq) vs AgCl/Ag at scan rates from 10 to 50 mV/s. (b) Linear variation in the anodic and cathodic peak current with the square root of the scan rate. The active electrode surface area is 10 cm^2.

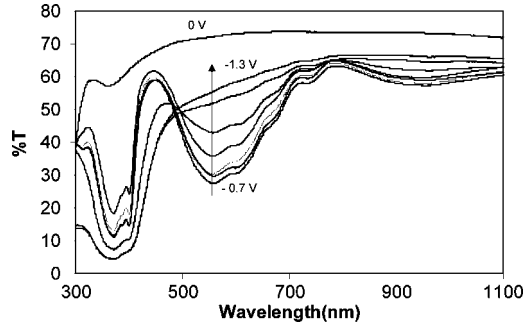

FIGURE 7. UV−vis spectra of 40-bilayer PXV NPs/PAMPS films in 0.1 M $NaClO_4$(aq) at 0 V and increasing voltage from −0.7 to −1.3 V, in 0.1 V steps.

electrolyte solution, and the film fairly quickly (within 3−4 s) loses its color as soon as the voltage is discontinued.

Transmission Spectra for Solid-State Devices. The transmission spectrum of the $(PXV\ NPs/PAMPS)_{40}$/$PAMPS/(PANI/PAMPS)_{40}$ device is presented in Figure 8 at 0 and 1−3 V (with respect to a PANI/PAMPS electrode) applied with a step increment of 0.5 V, as measured with a Filmetrics

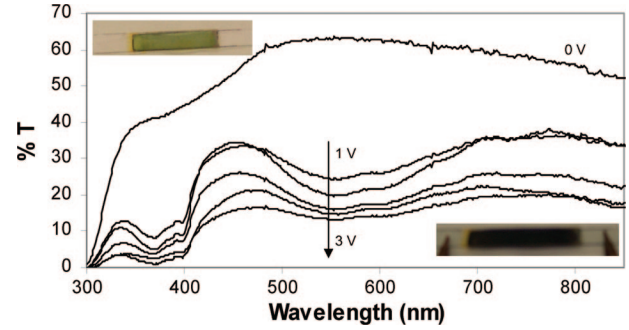

FIGURE 8. Transmission spectra from 0 to 3 V of a solid-state device fabricated by sandwiching two ITO electrodes coated with 40 bilayers of PXV NPs/PAMPS and PANI/PAMPS. Inset: solid-state device changing color from yellow-green to dark purple-blue.

F20 UV−vis spectrometer. The maximum contrast observed between the 0 and 3 V spectra is 50% at 550 nm. There have been several reports of all-solid-state electrochromic devices (10−18). The present work describes a device with the highest contrast ratio for comparable switching times. The matching contrast peak obtained at 550 nm for a solid-state device with the salt electrolyte solution confirms the color change of polyviologen NPs and not PANI; in addition, the solid-state device of PANI shows a peak at 490−500 nm (48). On application of + 0.6V and higher, PANI achieves its second oxidation state, which is yellow in color and hence does not contribute in dark purple-blue color of the solid-state device (50).

Unlike conducting polymer-based devices, it is not possible to fabricate symmetric solid-state devices (54) in the case of bipyridinium systems. As a cathodically coloring material, it is required to have an anodically coloring material like PANI to balance the flow of electrons. Solid-state switching of the 40-bilayer film of PXV NPs/PAMPS as the working electrode and PANI/PAMPS as the counter electrode shows switching times of 3 and 3.5 s for coloration and decoloration for a device size of 1 cm^2. As shown in Figure 9, the temporal response of the device for a color change from transparent yellow to deep purple-blue was monitored with a He−Ne laser (633 nm), and a photodiode as a square-wave voltage (0−3 V) was applied to the electrochromic device. There have been a few examples of solid-state devices (47, 49, 55) in the past few years, but this is by far the highest contrast (∼45% at 633 nm) thin film device with comparable switching speeds reported so far.

CONCLUSION

In this report, we have presented the changes that can occur by a small structural variation of the chain end groups of polyviologen; they affect the solubility, electrochromic and device properties of the material. The presence of a substitutent with silsesquioxane groups on the viologen gives water-dispersed NPs, which improves the film morphology without affecting the electrochromic properties of viologens. The LbL films of PXV NPs exhibit high contrast (ΔT = ∼50% under dynamic condition) with fairly fast switching in the solid state (∼3 s). The low reduction potential (−0.7 V) allows the LbL films to be switched between the PXV monoreduced

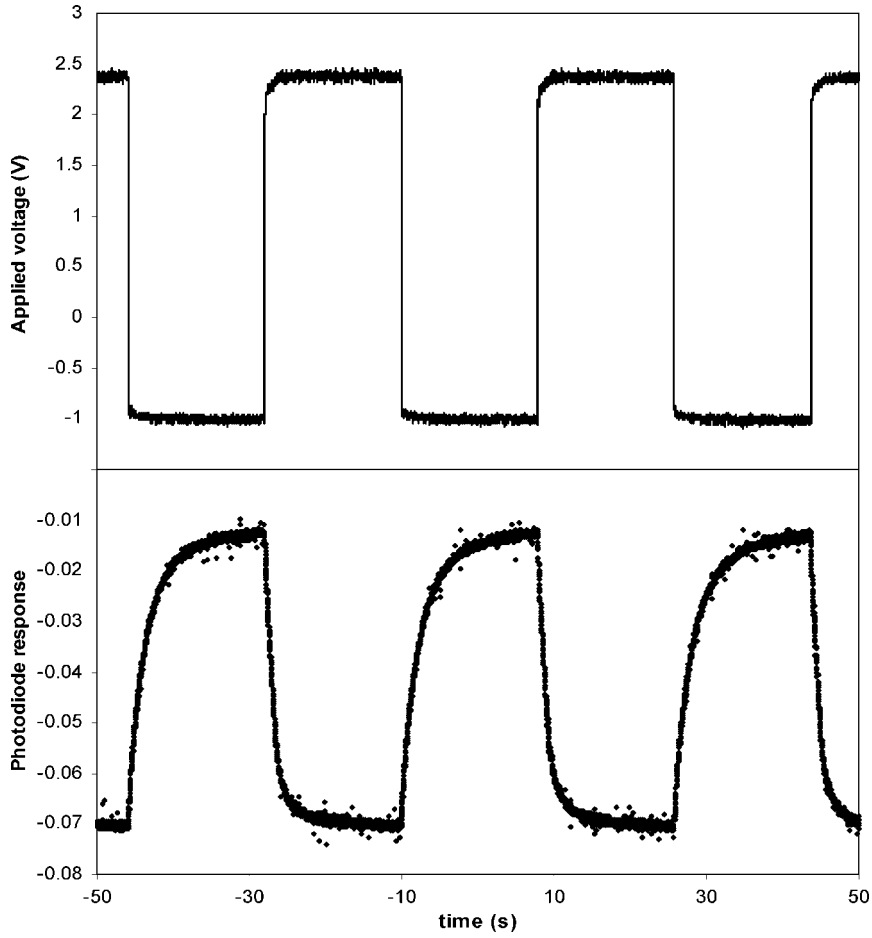

FIGURE 9. Switching in an asymmetric solid-state device (1 cm^2) at 633 nm upon application of a square-wave potential between 0 and 3 V.

and oxidized states. Because of the flexibility of the LbL assembly method, we note the potential to fabricate multihue electrochromic devices by combining anionic PEDOT and its derivatives with cationic PXV NPs. The combination of PXV NPs with other water-soluble anionic polyelectrolytes (both electrochromic and inactive) is still in progress, and the detailed study of their effect on the film thickness, contrast, and switching speed will be presented in our upcoming publications.

EXPERIMENTAL SECTION

Materials. Poly[2-(acrylamido)-2-methylpropanesulfonic acid] (PAMPS, Aldrich), polyaniline (PANI) in an emeraldine base form (Aldrich), sodium carbonate, magnesium sulfate, anhydrous sodium sulfate, calcium chloride, anhydrous potassium carbonate, NaOH, and concentrated HCl were used as received.

Equipment. An EG&G 273 A potentiostat/galvanostat was used for CV studies. For electrochemical characterization, an ITO-coated glass slide was used as the working electrode, a platinum wire as the counter electrode, and AgCl/Ag (3 M KCl) as the reference electrode. An automated dipping machine from Nanostrata Inc. was used for deposition of the multilayer films. ITO glass substrates (8−12 Ω) with dimensions 3 in. × 1 in. were bought from Delta Technologies. SEM images of the coated surface were taken on a LEO 1550 field emission scanning electron microscope at an accelerating voltage of 5 kV. AFM images were taken by Nanoscope IVa, and all of the imaging was done in tapping mode with a cantilever of 50 N/m force constant and an image size of 2 μm × 2 μm and 0−60 nm z-scale. SEM for NPs was performed on a ZEISS ULTRA 55 CDS ultrahigh-resolution field emission scanning electron microscope. NPs were drop-coated onto silicon wafers from water suspensions and dried overnight under ambient conditions. The typical accelerating voltage used was 5 kV. TEM was performed on a Philips CM20 TEM with an EDS (EDAX/4pi) system with a liquid-nitrogen holder. NP samples were dispersed in water, and drops of the resulting mixture were deposited on a plasma-etched amorphous carbon substrate supported copper grid and allowed to dry prior to imaging. Light scattering experiments were carried out on a Horiba LB-550 dynamic light scattering particle size analyzer. ζ potential measurements were performed by Malvern Zeta Nanosizer.

Film Fabrication and Characterization. LbL film fabrication (Scheme 1) was performed with the help of an automated slide strainer. The ITO substrates were washed with water to develop some negative charge and then exposed to a polyviologen NP (pH 4, 2 mg/mL) solution for 6 min, followed by three steps of rigorous rinsing with deionized water for 45 s. Finally, the substrates were exposed to a PAMPS (pH 4, 2 mM) solution for 6 min and again rinsed with water for 45 s each in three consecutive water baths. This cycle was repeated 40 times to get the desired number of bilayers. The pH of the solutions was adjusted with sodium hydroxide or hydrochloric acid. The PANI solution (pH 3.5) was prepared with an aqueous cosolvent including dimethylacetamide at a 10 mM polymer as described by Rubner et al. (56) LbL deposition of PANI/PAMPS films was done in a fashion similar to that for PXV NPs/PAMPS. The film thickness per bilayer of multilayer assemblies lies roughly in the range of 45−48 nm.

Acknowledgment. Mariya Khiterer thanks Lawrence Livermore National Laboratory for a graduate fellowship. H. M. Yochum acknowledges support from the *Sweet Briar Faculty Fellowship*.

REFERENCES AND NOTES

(1) Monk, P. M. S.; Mortimer, R. J.; Rosseinsky, D. R. *Electrochromism and Electrochromic Devices*; Cambridge University Press: Cambridge, U.K., 2007.
(2) Monk, P. M. S. Electrochromism in Viologen-based Systems. In *The Viologens. Physicochemical Properties, Synthesis and Applications of the Salts of 4,4′-Bipyridine*; John Wiley and Sons: New York, 1998; pp 239−258.
(3) Bookbinder, D. C.; Wrighton, M. S. *J. Electrochem. Soc.* **1983**, *130*, 1080.
(4) Barltrop, J. A.; Jackson, A. C. *J. Chem. Soc., Perkin Trans. 2* **1984**, 367.
(5) Mortimer, R. J.; Dyer, A. L.; Reynolds, J. R. *Displays* **2006**, *27*, 2.
(6) Bach, U.; Corr, D.; Lupo, D.; Pichot, F.; Ryan, M. *Adv. Mater.* **2002**, *14*, 845.
(7) Lee, S. H.; Deshpande, R.; Parilla, P. A.; Jones, K. M.; To, B.; Mahan, A. H.; Dillon, A. C. *Adv. Mater.* **2006**, *18*, 763.
(8) Choi, S. Y.; Mamak, M.; Coombs, N.; Chopra, N.; Ozin, G. A. *Nano Lett.* **2004**, *4*, 1231.
(9) Aliev, A. E.; Shin, H. W. *Solid State Ionics* **2002**, *154*, 425.
(10) Khiterer, M.; Shea, K. J. *Nano Lett.* **2007**, *7*, 2684.
(11) Ryu, J. H.; Shin, D. O.; Suh, K. D. *J. Polym. Sci., Part A: Polym. Chem.* **2005**, *43*, 6562.
(12) Cen, L.; Neoh, K. G.; Kang, E. T. *Adv. Mater.* **2005**, *17*, 1656.
(13) Ryu, J. H.; Lee, Y. H.; Suh, K. D. *J. Appl. Polym. Sci.* **2008**, *107*, 102.
(14) Ryu, J. H.; Lee, Y. H.; Han, S. H.; Suh, K. D. *Macromol. Rapid Commun.* **2007**, *27*, 1156.
(15) Wang, Z.; Hu, X. *Thin Solid Films* **1999**, *352*, 62.
(16) Papaefthimiou, S.; Leftheriotis, G.; Yianoulis, P. *Ionics* **1998**, *4*, 321.
(17) Stejskal, J.; Trchova, M.; Fedorova, S.; Sapurina, I.; Zemek, J. *Langmuir* **2003**, *19*, 3013.
(18) Curtis, C. L.; Ritchie, J. E.; Sailor, M. J. *Science* **1993**, *262*, 2014.
(19) Stepp, J.; Schlenoff, J. B. *J. Electrochem. Soc.* **1997**, *144*, L155.
(20) Delongchamp, D. M.; Kastantin, M.; Hammond, P. T. *Chem. Mater.* **2003**, *15*, 1575.
(21) Decher, G.; Hong, J. D.; Schmitt, J. *Thin Solid Films* **1992**, *1*, 831.
(22) Haas, H.; Decher, G.; Mohwald, H.; Kalacbevt, A. *J. Phys. Chem.* **1993**, *97*, 12835.
(23) Kotov, N. A.; Dekany, I.; Fendler, J. H. *J. Phys. Chem.* **1995**, *99*, 13605.
(24) Caruso, F.; Caruso, R. A.; Mohwald, H. *Science* **1998**, *282*, 1111.
(25) Feldheim, D. L.; Grabar, K. C.; Natan, M. J.; Mallouk, T. E. *J. Am. Chem. Soc.* **1998**, *118*, 7640.
(26) Lvov, Y.; Ariga, K.; Onda, M.; Ichinose, I.; Kunitake, T. *Langmuir* **1997**, *13*, 6195.
(27) Decher, G. *Science* **1997**, *227*, 1232.
(28) Shea, K. J.; Loy, D. A. *Chem. Mater.* **2001**, *13*, 3306.
(29) Shea, K. J.; Loy, D. A.; Webster, O. *J. Am. Chem. Soc.* **1992**, *114*, 6700.
(30) Shea, K. J.; Loy, D. A. *Polym. Mater. Sci. Eng.* **1990**, *63*, 281.
(31) Shea, K. J.; Moreau, J.; Loy, D. A.; Corriu, R. J. P.; Bour, B. Bridged Polysilsesquioxanes. Molecular-Engineering Nanostructured Hybrid Organic−Inorganic Materials. *Functional Hybrid Materials*; Wiley Interscience: New York, 2004; pp 50−85.
(32) Choi, K. M.; Shea, K. J. *Photonic Polymer Synthesis*; Marcel Dekker: New York, 1998; pp 437−480.
(33) Innocenzi, P.; Lebeau, B. *J. Mater. Chem.* **2005**, *15*, 3821.
(34) Kagan, C. R.; Mitzi, D. B.; Dimitrakopoulos, C. D. *Science* **1999**, *286*, 945.
(35) Oviatt, H. W.; Shea, K. J.; Kalluri, S.; Shi, Y. Q.; Steier, W. H.; Dalton, L. R. *Chem. Mater.* **1995**, *7*, 493.
(36) Shea, K. J.; Hobson, S. T. *J. Hybrid Organic/Inorganic Absorbents* **2003**.
(37) Liu, J.; Feng, X. D.; Fryxell, G. E.; Wang, L. Q.; Kim, A. Y.; Gong, M. L. *Adv. Mater.* **1998**, *10*, 161–165.
(38) Mercier, L.; Pinnavaia, T. J. *Adv. Mater.* **1997**, *9*, 500–503.
(39) Huang, G. T. *Technol. Rev.* **2005**, *108*, 64–67.
(40) Khiterer, M.; Loy, D. A.; Cornelius, C. J.; Fujimoto, C. H.; Small, J. H.; McIntire, T. M.; Shea, K. J. *Chem. Mater.* **2006**, *18*, 3665.
(41) Honma, I.; Takeda, Y.; Bae, J. M. *Solid State Ionics* **1999**, *120*, 255.
(42) Xiong, S.; Xiao, Y.; Ma, J.; Zhang, L.; Lu, X. *Macromol. Rapid Commun.* **2007**, *28*, 281.
(43) Santra, S.; Bagwe, R. P.; Dutta, D.; Stanley, J. T.; Walter, G. A.; Tan, W.; Moudgil, B. M.; Mericle, R. A. *Adv. Mater.* **2005**, *17*, 2165.
(44) Barbe, C. B.; John, K.; Linggen, F.; Kim, L.; Qiang, H.; Michael, L.; Sandrine, C.; Bush, A.; Calleja, G. *Adv. Mater.* **2004**, *16*, 1959.
(45) Bookbinder, D. C.; Wrighton, M. S. *J. Electrochem. Soc.* **1983**, *130*, 1080.
(46) Delongchamp, D. M.; Hammond, P. T. *Adv. Funct. Mater.* **2004**, *14*, 224.
(47) Jain, V.; Yochum, H. M.; Wang, H.; Montazami, R.; Hurtado, M. A. v.; Mendoza-Galvń, A.; Gibson, H. W.; Heflin, J. R. *Macromol. Chem. Phys.* **2008**, *209*, 150.
(48) Janik, J. A.; Heflin, J. R.; Marciu, D.; Miller, M. B.; Wang, H.; Gibson, H. W.; Davis, R. M. *Proc. Int. Soc. Opt. Eng.* **2001**, *4458*, 146.
(49) Jain, V.; Yochum, H. M.; Wang, H.; Montazami, R.; Heflin, J. R. *Appl. Phys. Lett.* **2008**, *92*, 033304.
(50) Delongchamp, D. M.; Hammond, P. T. *Adv. Mater.* **2001**, *13*, 1455.
(51) Ock, J.; Shin, H.; Kwon, Y.; Miyake, J. *Colloids Surf. A* **2005**, *351*, 257–258.
(52) Cutler, C. A.; Bouguettaya, M.; Kang, T.; Reynolds, J. R. *Macromolecules* **2005**, *38*, 3068.
(53) Cutler, C. A.; Bouguettaya, M.; Kang, T.; Reynolds, J. R. *Adv. Mater.* **2002**, *14*, 684.
(54) Mecerreyes, D.; Marcilla, R.; Ochoteco, E.; Grande, H.; Pomposoa, J. P.; Vergaz, R.; Pena, J. M. S. *Electrochim. Acta* **2004**, *49*, 3555.
(55) Jain, V.; Sahoo, R.; Jinschek, J. R.; Montazami, R.; Yochum, H. M.; Beyer, F. L.; Kumar, A.; Heflin, J. R. *Chem. Commun.* **2008**, 3663.
(56) Rubner, M. F.; Cheung, J. H.; Stockton, W. B. *Macromolecules* **1997**, *30*, 2712.

AM8000264